

Published in final edited form as:

*Cytokine*. 2013 October ; 64(1): 362–369. doi:10.1016/j.cyto.2013.05.015.

## Cytokines are systemic effectors of lymphatic function in acute inflammation

Melissa B. Aldrich<sup>a,\*</sup> and Eva M. Sevick-Muraca<sup>a</sup>

<sup>a</sup>The Center for Molecular Imaging, Brown Foundation Institute for Molecular Medicine, The University of Texas Health Science Center-Houston, 1825 Pressler, 330-07, Houston, Texas 77030

### Abstract

The response of the lymphatic system to inflammatory insult and infection is not completely understood. Using a near-infrared fluorescence (NIRF) imaging system to noninvasively document propulsive function, we noted the short-term cessation of murine lymphatic propulsion as early as four hours following LPS injection. Notably, the effects were systemic, displaying bilateral lymphatic pumping cessation after a unilateral insult. Furthermore, IL-1, TNF- $\alpha$ , and IL-6, cytokines that were found to be elevated in serum during lymphatic pumping cessation, were shown separately to acutely and systemically decrease lymphatic pulsing frequency and velocity following intradermal administration. Surprisingly, marked lymphatic vessel dilation and leakiness were noted in limbs contralateral to IL-1 intradermal administration, but not in ipsilateral limbs. The effects of IL-1 on lymphatic pumping were abated by pretreatment with an inhibitor of inducible nitric oxide synthase, L-NIL (N-iminoethyl-L-lysine). The results suggest that lymphatic propulsion is systemically impaired within four hours of acute inflammatory insult, and that some cytokines are major effectors of lymphatic pumping cessation through nitric oxide-mediated mechanisms. These findings may help in understanding the actions of cytokines as mediators of lymphatic function in inflammatory and infectious states.

### Keywords

lymphatic; inflammation; interleukin-1 beta; interleukin-6; tumor necrosis factor-alpha

## 1. Introduction

Inflammation is a response to pathogens, damaged cells, or irritation, resulting from infection, injury, autoimmune pathologies, or stress [1]. Cardiovascular and immune system responses to inflammation and infection are well documented, but the role of the lymphatic system is illdefined, largely due to a lack of tools for studying the system. Responsible for fat absorption in the gut, and for transport of excess fluid, macromolecules, and cellular debris from the interstitial space to the hemovascular system, the lymphatics also play a critical role in mediating the immune response [2, 3]. An imaging technique for noninvasively visualizing lymphatic vessel structure and function [4–6] now allows for

© 2013 Elsevier Ltd. All rights reserved.

Corresponding author Melissa.B.Aldrich@uth.tmc.edu, Phone number: 1-713-500-3565, FAX number: 1-713-500-0319.

**Publisher's Disclaimer:** This is a PDF file of an unedited manuscript that has been accepted for publication. As a service to our customers we are providing this early version of the manuscript. The manuscript will undergo copyediting, typesetting, and review of the resulting proof before it is published in its final citable form. Please note that during the production process errors may be discovered which could affect the content, and all legal disclaimers that apply to the journal pertain.

investigation of the systemic response of the lymphatic circulatory system in infection and inflammation.

One model used for studying inflammation caused by exogenous pyrogens includes the use of lipopolysaccharide (LPS), a cell wall component of gram-negative bacteria. LPS binds to the CD14/TLR4/MD2 complex on many cells, especially macrophages, and results in signaling cascades directing the synthesis and release of cytokines, such as interleukin 1 (IL-1), interleukin 6 (IL-6), and tumor necrosis factor-alpha (TNF- $\alpha$ ) [7]. The role that these cytokines and other molecular signals play in affecting lymphatic fluid and immune cell transport as part of the immune response is incompletely understood.

Although lymphangiogenesis is a well documented response to inflammation [8–13], not enough is known about the role of lymphatic transport in mediating and resolving inflammatory responses. The timely orchestration of lymph flow and cell movement within lymphatic vessels during different types of inflammatory events has yet to be thoroughly described. For example, dendritic cell (DC) and other immune cell transport to lymph nodes increases in response to chemokines expressed during inflammatory insults, yet some studies report a slowdown in lymph movement [14–17]. Most studies of lymphatic transport have reported effects using different inflammation models at limited time points or only in the local physiological environment surrounding the inflammatory insult [18–22]. A clear, macroscopic picture of systemic, temporal responses of lymph movement in acute, chronic, Th1-type (T helper 1-type), Th2-type, and Th17-type inflammation, together with information on the machinations of immune cell migration, is presently lacking.

In this study, using noninvasive, near-infrared fluorescence imaging (NIRF), we show transient changes in lymphatic transport in response to acute inflammation caused by unilateral LPS injection in the dorsal aspect of the hind paw in mice. We observed early, severe retardation of lymphatic pumping in response to a unilateral inflammatory insult, and, surprisingly, noted that the effect was systemic (bilateral)—not exclusively local. Additionally, we noted decreased systemic lymphatic propulsion after separate injection of IL-6, TNF- $\alpha$ , and IL-1 $\beta$ , cytokines that are elevated in serum after LPS injection, indicating that these cytokines may play an important role in control of lymphatic function. Curiously, distal contralateral lymphatic vessels were dilated and leaky after IL-1 $\beta$  treatment, while ipsilateral vessels were not. The action of IL-1 $\beta$  on lymphatic pumping was mitigated by inhibition of inducible nitric oxide synthase (iNOS), suggesting that cytokine effects on systemic lymphatic function in acute inflammation are driven by nitric oxide production.

## 2 Materials and Methods

### 2.1 Mice

10–12 weeks-old female mice were obtained from Charles River (Wilmington, MA) and housed in an Association for Assessment and Accreditation of Laboratory Animal Care-approved facility, according to institutional guidelines. All animal protocols were reviewed and approved by the Institutional Animal Care and Use Committee at the University of Texas Health Science Center-Houston. Female mice were used, as males tended to induce fight wounds on skin that diminished imaging quality. Mice were not tattooed, since tattooing can induce inflammation that lasts 14 days or more [23]. Mice were, however, eartagged several weeks before first imaging.

### 2.2 Reagents

Indocyanine green (ICG) was obtained from Akorn, Inc. (Lake Forest, IL) and diluted with sterile saline (Hospira, Lake Forest, IL) to 625  $\mu$ M for use. Lipopolysaccharide (LPS) was purchased from Sigma-Aldrich (#L 3024, *E. coli* serotype 0111:B4, purified by ion

exchange). Recombinant murine TNF- $\alpha$ , IL-1 $\beta$ , IL-1 $\alpha$ , interferon-gamma (IFN- $\gamma$ ), monocyte chemoattractant protein-1/chemokine (C-C motif) ligand 2 (MCP-1/CCL2), and IL-6 were purchased from Peprotech (Rocky Hill, NJ). Recombinant human vascular endothelial growth factor-C (VEGF-C) was purchased from R&D Systems (Minneapolis, MN). L-NIL (N-iminoethyl-L-lysine) was purchased from Sigma-Aldrich.

### 2.3 LPS and cytokine injection

Mice were anesthetized with isoflurane, shaved, and covered with depilatory cream (Nair Sensitive) for three minutes. The cream was then rinsed off with warm water. Several days later, mice were anesthetized with isoflurane, and 10  $\mu$ L of 625  $\mu$ M ICG were injected intradermally with a 31-gauge needle/syringe (BD #328438, Fisher Scientific) at the base of the tail and/or on the dorsal side of the paw on both right and left sides of the mice to perform baseline NIRF imaging of the lymphatics. Two-three days after this initial imaging, mice were injected intradermally with 20  $\mu$ L of 5 mg/mL (100  $\mu$ g/mouse) of bacterial wall lipopolysaccharide, saline, or TNF- $\alpha$  (2  $\mu$ g/mouse), IL-6 (50 ng/mouse), and/or IL-1 $\beta$  (1  $\mu$ g/mouse) in saline in the dorsal aspect of the right hind paw. In separate experiments, interferon-gamma (IFN- $\gamma$ , 400 ng/mouse), interleukin-1 alpha (IL-1 $\alpha$ , 0.5  $\mu$ g/mouse), monocyte chemoattractant protein-1/chemokine (C-C motif) ligand 2 (MCP-1/CCL2, 0.8  $\mu$ g/mouse), and vascular endothelial growth factor-C (VEGF-C, 400 ng/mouse) were injected intradermally in the dorsal aspect of the right hind paw. The cytokine amounts were chosen based on previously published inflammatory or other effects [24–42]. In some experiments, TNF- $\alpha$  and IL-1 $\beta$  were heat-inactivated (85°C, 15 minutes), in order to affirm that residual LPS in the cytokine materials did not account for effects observed [43–46].

### 2.4 Near-infrared fluorescent lymphatic imaging

NIRF images were collected with a custom-built system that employed illumination of tissue surfaces with 785-nm light from a laser diode (85 mA and 80 mW, DL7140–201, Sanyo) that was diffused to cover a circular area of approximately 8 cm in diameter [4, 6]. Fluorescent light generated from the ICG within the lymphatic vasculature was collected with an EMCCD camera (electron-multiplying charge-coupled device, model 7827-0001, Princeton Instruments). Filter sets were used to reject backscattered and reflected excitation light. Images were acquired with V++ software (Total Turnkey Solutions, Sydney, Australia). The integration time for fluorescence images was 200 milliseconds. 300 images were collected per side per mouse for lymph velocity and propulsive frequency measurements. Images were collected at zero and four hours, and also at one, two, four, and seven days after LPS injection. Images were collected at four hours after cytokine treatment with or without previous injection of iNOS inhibitor. In separate experiments, images were collected at 30, 60, 90, and 120 minutes after LPS or IL-1 $\beta$  injection, in order to compare kinetics of effects on lymphatic pumping.

### 2.5 Data analysis/statistics

Images were loaded into ImageJ software (NIH), and fluorescence intensity values were quantified and imported into Microsoft Excel for computation of propulsive frequencies and velocities as previously described [6]. Statistical significance for comparisons of propulsive frequencies was determined using ANOVA. Statistical significance for comparisons of propulsive velocities was determined using a linear mixed effects model.

### 2.6 Multiplex analysis of serum cytokines

Serum samples were obtained by retro-orbital bleeds of mice before LPS or saline injection, as well as at 1 day, 2 days, and 7 days post-injection (only one sample was collected per mouse). Approximately 200  $\mu$ L blood per mouse was left at room temperature for 30

minutes to allow coagulation, and then spun at 350 x g for 10 minutes at room temperature. Serum was collected and stored at  $-80^{\circ}\text{C}$  until analysis. For multiplex analysis, serum samples were diluted and processed according to manufacturer's instructions (Millipore catalog #MPXMCYP2-73K-02 [MCP-5, IL-25], #MPXMCYTO-70K-15 [GM-CSF, IFN- $\gamma$ , IL-1 $\beta$ , IL-1 $\alpha$ , IL-2, IL-3, IL-4, IL-6, IL-10, IL-12p40, IL-17, MCP-1, RANTES, TNF- $\alpha$ , VEGF], #MPXMCYP3-74K-02 [IL-25, IL-27], and #MSCR-42K-03 [mVEGFR1, mVEGFR2, mVEGFR3]). Cytokine/chemokine levels were measured on a Luminex 200 instrument (Millipore, Billerica, MA).

## 2.7 Vessel dilation measurement

Four hours after dorsal i.d. cytokine (1  $\mu\text{g}$  of IL-1 $\beta$ ) injection in the right or left hind paw, mice were anesthetized with isoflurane, 1% Evan's blue dye was injected i.d. at the base of the tail and in the dorsal paw areas, and inguinal-to-axillary and hind limb lymphatic vessels were photographed to record vessel dilation (Leica M165 microscope with a DFC2990 camera). Vessel diameters from intravital images were measured using ImageJ software.

## 2.8 Lymphatic endothelial cell (LEC) culture and nitric oxide (NO) measurement in culture supernatant

LECs (ScienCell, San Diego, CA, passage 8),  $1 \times 10^6$  cells/well in 12-well plates, were established in endothelial cell medium and then rinsed and cultured in Dulbecco's Modified Essential Medium (DMEM) with 10% fetal bovine serum and 1% penicillin/streptomycin for 12 hours after addition of cytokines. (Endothelial cell medium contains cortisone, which inhibits nitric oxide production.) LPS (1  $\mu\text{g}/\text{ml}$ ), TNF- $\alpha$  (20  $\text{ng}/\text{mL}$ ), IL-1 $\beta$  (10  $\text{ng}/\text{mL}$ ), IL-6 (1  $\text{ng}/\text{mL}$ ), or IL-6 plus IL-1 $\beta$  were added to wells of LECs, as well as to control wells containing RAW 264.7 macrophages, a gift from Dr. Nathan Bryan. Cytokine concentrations were chosen according to published stimulatory cell culture effects [47–49]. At 0, 6, and 12 hours [50] after cytokine addition, 100  $\mu\text{L}$  aliquots of cell culture medium per well were removed and stored at minus  $20^{\circ}\text{C}$ . Supernatant nitric oxide levels were measured by a Greiss reagent system (G2930, Promega, Madison, WI).

## 2.9 Inducible nitric oxide synthase inhibition in vivo

Mice were injected i.p. with 200  $\mu\text{g}$  of the iNOS inhibitor L-NIL (N[6]-(1-iminoethyl)-L-lysine) in 20  $\mu\text{L}$  saline. This dose was selected based on previously reported attenuation of inflammation and edema [51]. One hour later, these mice were injected intradermally in the dorsal aspect of the right hind feet with IL-1 $\beta$  (1  $\mu\text{g}/\text{mouse}$  in 20  $\mu\text{L}$  saline) or saline. Four more hours later, these mice were imaged with ICG injected at the base of tails, and lymphatic pulsatile velocity and frequency were recorded.

## 3. Results

### 3.1 Systemic lymph velocity and lymph propulsive frequency decreased after LPS administration

Figure 1 shows still images of normal fluorescent lymph movement along an inguinal-to-axillary collecting lymphatic vessel. A bolus of lymph, marked by arrows, can be seen moving up the vessel as time progresses, at an average rate of  $\sim 0.7$  centimeters per second and at a frequency of  $\sim 7$  pulses per minute, in untreated or saline-injected mice. Supplementary Videos 1 and 2 show, respectively, movies of lymph moving along the right side of a mouse injected with saline (inguinal-to-axillary lymph flow) and not moving along the left side of a mouse injected with LPS (LPS injection was on the right side). Marked decreases in systemic lymph propulsive velocity and propulsive frequency were noted within four hours after LPS administration. Figure 2 summarizes average lymph propulsive

velocities and propulsive frequencies at different time points after LPS injection. Lymph propulsive velocity and propulsive frequency approached zero at four hours post-LPS treatment, remained at levels of less than half of normal for the first two days, and then approached normal values by seven days after LPS treatment. Surprisingly, inguinal-to-axillary peripheral lymphatic vessels on both left and right sides of the mice exhibited reduced lymphatic function, even though only the right hind paw was injected with LPS, thus displaying systemic, early response to inflammation.

### 3.2 Cytokine/chemokine levels increased with LPS administration

The dramatic change in lymphatic propulsive velocity at early time points after LPS injection suggested a systemic signal rapidly affecting lymphatic pumping function. Serum cytokine and chemokine concentrations were evaluated, to determine if these levels correlated with the rates of lymphatic propulsion. Of the serum cytokines and chemokines measured, the levels of TNF- $\alpha$ , IL-6, IL-1 $\beta$ , MCP-1/CCL2, RANTES, MCP-5/CCL12, IL-10, IL-12p40, IL-17, IFN- $\gamma$ , and GM-CSF significantly increased ( $p < 0.05$ ) four hours after LPS injection. Figure 3 shows values for TNF- $\alpha$ , IL-6, and IL-1 $\beta$  (other increased cytokine values are shown in Supplementary Figure 1). Variability in mouse serum samples was seen in large standard deviations within groups. Other cytokines measured were sVEGF, IL-1 $\alpha$ , IL-4, IL-25, IL-2, IL-3, sVEGFR-1, sVEGFR-2, and sVEGFR-3, all of which did not increase significantly within the first two days after LPS treatment (data not shown).

### 3.3 Lymphatic function changed with cytokine injection

From these results, we hypothesized that a soluble factor delivering a systemic signal to the lymphatic system could be one or more of the observed elevated cytokines. To test the ability of cytokines to directly affect systemic lymphatic function, selected cytokines were injected intradermally in the dorsal aspect of the right hind paw, and lymphatic function was assessed by NIRF imaging. IL-6, IL-1 $\beta$ , and TNF- $\alpha$  were chosen, due to their serum elevation after LPS and their reported effects on blood vasculature dilation in inflammation [52]. Lymphatic pulses per minute on both sides of the mice, as shown in Figure 4a, significantly decreased ( $p < 0.05$ ) with TNF- $\alpha$ , IL-6, IL-1 $\beta$ , and IL-6 plus IL-1 $\beta$  injection, compared to saline injection controls. Lymphatic pulsatile velocities (Figure 4b) significantly decreased ( $p < 0.05$ ) with injection of IL-1 $\beta$  (contralateral side) and IL-6 plus IL-1 $\beta$  (both sides), compared to saline injection controls. As a test of other families of cytokines or chemokines, IFN- $\gamma$ , MCP-1/CCL2, IL-1 $\alpha$ , and VEGF-C were injected in right hind paws, and none of these agents slowed lymph pumping at 4 hours (Supplementary Figure 2). Heat-inactivated TNF- $\alpha$  and IL-1 $\beta$  did not affect lymphatic pumping (Supplementary Figure 3), and LPS and IL-1 $\beta$  effects followed similar kinetic trajectories (Supplementary Figure 4). Large variations between mice resulted in large standard deviations within groups. Surprisingly, some of the IL-1 $\beta$ -treated mice exhibited backwards flow (Supplementary Video 3), which was recorded as zero pulses per minute. IL-1 $\beta$  was used in subsequent experiments to further test the cytokine's effects on lymphatics.

### 3.4 Contralateral hind limb, but not inguinal-to-axillary lymphatic or ipsilateral hind limb, vessels were dilated or leaky with IL-1 $\beta$ treatment

Lymphatic pulsing could be disrupted by dilated or leaky vessels. Lymphatic vessel dilation was investigated by taking intravital images of inguinal-to-axillary lymphatic vessels and hind limb vessels containing Evan's blue dye 4 hours after i.d. dorsal paw injection of IL-1 $\beta$  in mice (Figure 5a and b). Curiously, lymphatic vessels in the hind limbs contralateral to the cytokine injection appeared significantly more dilated and leaky, as quantified by vessel/dye diameter, after IL-1 $\beta$  injection (Figure 5c). Ipsilateral hind limb vessels, however, did not

appear dilated or leaky after IL-1 injection. Inguinal-to-axillary lymphatic vessels on both sides displayed slightly increased diameters in response to IL-1.

### 3.5 Nitric oxide production by LECs cultured independently of other cell types did not increase with cytokine treatment

Lymphatic vessel dilation can be modulated by nitric oxide levels [53–56]. The ability of lymphatic endothelial cells to produce nitric oxide in response to cytokine stimulation was tested. Cultured LECs treated with TNF- $\alpha$ , IL-6, IL-1 $\beta$ , or IL-6 with IL-1 $\beta$  produced no nitric oxide that was detectable by the Greiss analysis system used (data not shown). LECs treated with LPS also did not produce measurable nitric oxide. RAW 264.7 macrophages used as control cells did produce nitric oxide in response to LPS stimulation, but did not produce NO in response to cytokine stimulation (TNF- $\alpha$ , IL-6, and IL-1 $\beta$  combined, data not shown).

### 3.6 iNOS inhibition restored lymphatic function after IL-1 $\beta$ stimulation

In order to discern if the systemic effects of IL-1 $\beta$  on lymphatic function in inflammation were mediated by nitric oxide, we injected an inhibitor of inducible nitric oxide (iNOS), before injecting IL-1 $\beta$ . Figure 6 shows that the reduction of lymphatic propulsive frequency and velocity imaged four hours following administration of IL-1 $\beta$  was abrogated when the iNOS inhibitor, L-NIL, was injected i.p. one hour before injection of IL-1 $\beta$ . Although large variations between mice resulted in large standard deviations within groups, significant differences from control animals (saline or L-NIL treatment only) in pulsatile frequency were only noted in IL-1 $\beta$ -treated animals with no L-NIL pre-treatment.

## 4. Discussion

We demonstrated that systemic lymph velocity and propulsive frequency dropped to near-zero values within four hours after LPS administration. This dramatic, rapid reduction in lymphatic propulsive flow and frequency, in a normally occurring inflammatory event, could act to prevent the spread of infectious or inflammatory agents beyond the region or lymph node needed for a localized immune response, as well as facilitate vascular wall adhesion and chemotaxis of lymphocytes. Reduced lymph movement could also facilitate evasion of the immune system by pathological agents and cancer cells. The slowdown of lymphatic propulsion after intradermal TNF- $\alpha$ , IL-6, and IL-1 $\beta$  injection suggests that cytokines produced in response to LPS were mediators of the observed systemic change in lymphatic function.

LECs, macrophages and other cells may have been the source of cytokine production in response to LPS. Indeed, cultured LECs treated with LPS upregulate mRNA for several cytokines [57]. Cytokines/chemokines could affect lymph function directly, or cause LECs, macrophages, or other cells, likely in cooperation, to release factors that influence lymphatic function. Local cytokine concentrations, which were not measured, may have varied in different anatomical locations. LPS-binding protein, cytokine receptor, and TLR expression levels vary on different cell types, so LPS or resulting autocrine/paracrine cytokine signaling may not be uniform [58]. Although the source and mechanism of cytokine/chemokine action on lymphatics are unknown, our results implicate these molecules as rapid, systemic effectors of lymph propulsion.

Of course, other molecular signals in inflammatory events besides cytokines and chemokines may be modulators of the decreased systemic lymph flow observed in the LPS acute inflammation model. For example, substance P activates the contractile pathway in cultured rat mesenteric lymphatic muscle cells [59], and heparin decreases bovine lymphatic

vessel contractions *via* nitric oxide production by endothelial cells [60]. Vasoactive intestinal peptide inhibits lymphatic pumping in mesenteric collecting lymphatic vessels [61]. Additionally, calcium levels in smooth muscle cells may, as in vascular tissue, regulate lymphatic vessel contractions [62]. Whether these facilitators of lymphatic function act downstream of cytokines in this model of inflammation remains to be investigated.

The observed systemic slowing or stoppage, as well as backwards flow, of lymph in response to inflammatory insults may result from dilation and presumed stagnant pooling of lymph in the afferent, efferent, intranodal, or internodal lymphatic vessels. TNF- $\alpha$  and IFN- $\gamma$  are potent stimulators of macrophage-produced nitric oxide, which has been shown to influence mesenteric lymphatic vessel contraction by dilatation [62, 63]. Nitric oxide may function as a causative, direct agent in lymphatic pumping, or may be an integral part of a loop of effectors [64, 65]. Indeed, iNOS expression in response to LPS can occur directly through F-kB signaling without the need for cytokine stimulation, and SPSB2, an adapter protein in the iNOS ubiquitin ligase complex, controls NO production in response to TLR signaling [66]. The rapid effect of LPS seen in this study could have occurred without cytokine release, because we observed very similar early kinetics of lymphatic pumping cessation with LPS and IL-1 $\beta$  (Supplementary Figure 4). It is also possible that pre-formed cytokines waiting for release from mast cells or other granulocytes allowed for very rapid cytokine secretion in response to LPS [67]. The effects of NO on lymphatic function are most likely complex and utilize redundant mechanisms. In response to LPS or cytokines, iNOS-driven nitric oxide production by lymphatic endothelial or other cells may drive lymphatic vessel dilation and lymphatic vessel smooth muscle inactivation that slows lymph movement.

Our observation of no discernible *in vitro* NO production by lymphatic endothelial cells in direct response to the cytokines TNF- $\alpha$ , IL-6, and IL-1 $\beta$  suggests that any cytokine-associated lymphatic vessel dilation may result from NO production by LECs only with cooperation from other cells, by cell types other than LECs, from complex cytokine/NO feedback interactions, or from mechanisms not directly connected to NO. Our *in vitro* results are in accord with a study demonstrating that *in vitro* LEC expression of nitric oxide synthase 2 (NOS2) and NO production requires a tripartite synergism of IFN- $\gamma$ , TNF, and direct LEC-T cell contact [63].

Injection of MCP-1/CCL2, a chemokine, interferon- $\gamma$ , a type II cytokine, as well as two cytokines that were not elevated 4 hours after LPS administration, VEGF-C and IL-1 $\beta$ , did not have any effect on lymphatic pumping at 4 hours (Supplementary Figure 2), suggesting that only a few cytokines affect lymphatic function in inflammatory conditions.

Other studies have reported changes in afferent, efferent, and intranodal blood and lymphatic vessel function in response to inflammation. Soderberg et al. observed that, several days after LPS injection in mouse paws, popliteal entry blood arterioles increased in diameter by 50%, due to vascular remodeling [68]. Liao, et al. noted decreased afferent lymph vessel function in draining lymph nodes 2–4 days after oxazolone treatment [69]. Wee, et al. injected IL-6 or TNF- $\alpha$  into draining areas of cannulated sheep lymph nodes and observed a unilateral shutdown phase with reduced efferent cell output, followed by a “recruitment” phase with elevated efferent cell output [17]. Our study, however, to our knowledge, is the first to document systemic, macroscopic, internodal lymphatic flow changes starting a few hours after initiation of insult and continuing through several days’ duration. This report shows that effects on the flow of lymph were not confined to the region of inflammatory insult.

Pumping directly affects “ejection” velocity, so we would expect to see lower velocity values after IL-1 treatment. Lymphatic pumping has been described as having intrinsic and extrinsic controllers. Extrinsic controllers respond to cyclical compression and expansion forces in surrounding tissue, while intrinsic pumps function due to rapid, phasic contractions of lymphatic muscle. Inflammation can allow iNOS produced by macrophages to “overwhelm” the normally fluctuating, local eNOS-produced NO gradients that control regular lymphatic pumping. There is always passive velocity for lymph flow (due to a positive pressure gradient, viscous lymph forces, and valve operation), while intrinsic and extrinsic factors contribute to pumping “ejection” velocity. The intrinsic pump-controlling muscle layer that is responsible for the regulation of lymphatic diameter is presumably altered in the dilated vessels that we observed (Figure 5). We did not observe significant overall effects on the velocity, possibly because iNOS may not affect passive flow, or iNOS may not completely affect intrinsic or extrinsic controllers of pumping, or passive velocity changes simply may not have been as dramatic as pumping frequency changes. Additionally, iNOS may not have significantly affected sympathetic and parasympathetic innervation of lymphatics that can control smooth muscle cell contraction of lymph vessels [70].

Intravital imaging of inguinal-to-axillary as well as lower hind limb lymphatics revealed obvious systemic vessel dilation and leakage primarily in contralateral hind limb lymphatic vessels. This observation, curiously, mimics the unaffected, contralateral arm lymphatic vessel dilation noted in human NIRF and lymphoscintigraphic imaging of many breast cancer-related lymphedema subjects with severely impaired lymphatic function on the affected side [71, 72]. Whether this contralateral dilation functions to compensate for restricted lymph flow or cell migration on the ipsilateral side is unknown, and is puzzling, given that the flow of lymph (or lack of flow) appears to be similar on both sides in our mouse model of inflammation.

Discrepancies between the results seen in this study and other studies could be attributed to measurements of different lymphatic vessels (i.e., inguinal-to-axillary *versus* mesenteric), route of LPS injection (i.d. *versus* i.v. or subcutaneous), time elapsed since inflammatory insult, and the fact that this study looked at bilateral/systemic, not only local, microscopic lymphatic responses. The inguinal-to-axillary lymphatic vessel imaged may not be representative of all lymphatic vessels, but was used in this study to easily compare control and inflamed systems on a macroscopic scale. It is possible that lymph movement noted in the inguinal-to-axillary vessels did not correlate with movement in more internal vessels, such as mesenteric, but inguinal-to-axillary movement did coincide with lymph movement in lymphatic vessel plexuses in the superficial hind flank areas.

## 5. Conclusions

This report shows temporal systemic shutdown and recovery of lymphatic function in a model of acute inflammation and in response to cytokines. While other studies have shown microscopic, cellular, and local lymphatic function changes in inflammation, this study provides pieces of “the big picture” needed to understand where and how lymph flows macroscopically under inflammatory conditions. Similar studies of lymph movement in different types of inflammation (Th2, Th17) would be of interest. Such studies could provide macroscopic, temporal observations of lymph propulsive velocities, flow directions, and vessel remodeling to direct optimal development and testing of therapeutics, vaccines, and diagnostics for inflammatory, cancerous, and infectious diseases.



## Supplementary Material

Refer to Web version on PubMed Central for supplementary material.

## Acknowledgments

This work was funded by DOD/DARPA seedling N66001-09-C-2052 and National Heart, Lung, and Blood Institute RO1 HL092923. Melissa Aldrich designed experiments, collected, analyzed, and interpreted data, and wrote and submitted the report. Eva Sevick-Muraca designed experiments and interpreted results. The authors would like to thank Germaine Agollah for assistance with cultured lymphatic endothelial cell experiments, Dr. Nathan Bryan for the macrophage cell line and help with *in vitro* nitric oxide experiments, Holly Robinson and Gabriel Dickinson for assistance with animal handling, Dr. Amy Hazen for flow cytometry assistance, and Dr. Wenyaw Chan for statistical analysis.

Grant support: DARPA seedling N66001-09-C-2052, RP 110776 from the Cancer Prevention and Research Institute of Texas (CPRIT), and National Heart, Lung, and Blood Institute RO1 HL092923

## Abbreviations

<b>NIRF</b>	near-infrared fluorescence imaging
<b>L-NIL</b>	lipopolysaccharide
<b>LPS</b>	inducible nitric oxide
<b>iNOS</b>	Th1-type
<b>T helper 1-type</b>	CD14/Toll-like receptor 4/MD2
<b>CD14/TLR4/MD2</b>	indocyanine green
<b>ICG</b>	lymphatic endothelial cells
<b>LECs</b>	monocyte chemoattractant protein-1/chemokine (C-C motif) ligand 2 (MCP-1/CCL2)
<b>IFN-</b>	interferon-gamma
<b>IL</b>	interleukin

## References

1. Stedman, TL. Stedman's Medical Dictionary. 28 th. Baltimore, Maryland: Lippincott Williams and Wilkins; 2006.
2. Alitalo K. The lymphatic vasculature in disease. *Nat Med.* 2011; 17:1371–1380. [PubMed: 22064427]
3. Wang Y, Oliver G. Current views on the function of the lymphatic vasculature in health and disease. *Gene Dev.* 2010; 24:2115–2126. [PubMed: 20889712]
4. Kwon S, Sevick-Muraca EM. Noninvasive quantitative imaging of lymph function in mice. *Lymphat Res Biol.* 2007; 5:219–231. [PubMed: 18370912]
5. Rasmussen JC, Tan I-C, Marshall MV, Adams KE, Kwon S, Fife CE, Maus EA, Smith LA, Covington KR, Sevick-Muraca EM. Human lymphatic architecture and dynamic transport imaged using near-infrared fluorescence. *Transl Oncol.* 2010; 3:362–372. [PubMed: 21151475]
6. Aldrich MB, Davies-Venn C, Angermiller B, Robinson H, Chan W, Kwon S, Sevick-Muraca EM. Concentration of ICG does not significantly influence lymphatic function as assessed by near-infrared imaging. *Lymphat Res Biol.* 2012; 10:1–6. [PubMed: 22439852]
7. Schromm AB, Howe J, Ulmer AJ, Wiesmuller KH, Seyberth T, Jung G, Rossie M, Koch MH, Gutsmann T, Brandenburg K. Physicochemical and biological analysis of synthetic bacterial lipopeptides: validity of the concept of endotoxic conformation. *J Biol Chem.* 2007; 282:11030–11037. [PubMed: 17308304]

8. Flister MJ, Wilber A, Hall KL, Iwata C, Miyazono K, Nisato RE, Pepper MS, Zawieja DC, Ran S. Inflammation induces lymphangiogenesis through upregulation of VEGFR-2 mediated by NF- $\kappa$ B and Prox1. *Blood*. 2010; 115:418–429. [PubMed: 19901262]
9. Kang S, Lee S-P, Kim KE, Kim H-Z, Memet S, Koh GY. Toll-like receptor 4 in lymphatic endothelial cells contributes to LPS-induced lymphangiogenesis by chemotactic recruitment of macrophages. *Blood*. 2009; 113:2605–2613. [PubMed: 19098273]
10. Kataru RP, Keehoon J, Cholsoon J, Hanseul Y, Schwendener RA, Baik JE, Han SH, Alitalo K, Koh GY. Critical role of CD11b<sup>+</sup> macrophages and VEGF in inflammatory lymphangiogenesis, antigen clearance, and inflammation resolution. *Blood*. 2009; 113:5650–569. [PubMed: 19346498]
11. Wilting J, Becker J, Buttler K, Weich HA. Lymphatics and inflammation. *Curr Med Chem*. 2009; 16:4581–4592. [PubMed: 19903150]
12. Halin C, Detmar M. Chapter 1. Inflammation, angiogenesis, and lymphangiogenesis. *Method Enzymol*. 2008; 445:1–25.
13. Kim H, Kataru RP, Koh GY. Regulation and implications of inflammatory lymphangiogenesis. *Trends Immunol*. 2012; 33:350–356. [PubMed: 22579522]
14. Lee KM, McKimmie CS, Gilchrist DS, Pallas KJ, Nibbs RJ, Garside P, McDonald V, Jenkins C, Ransohoff R, Liu L, Milling S, Cerovic V, Graham GJ. D6 facilitates cellular migration, and fluid flow, to lymph nodes by suppressing lymphatic congestion. *Blood*. 2011; 118:6220–6229. [PubMed: 21979941]
15. Angeli V, Randolph GJ. Inflammation, lymphatic function, and dendritic cell migration. *Lymphat Res Biol*. 2006; 4:217–228. [PubMed: 17394405]
16. Elias RM, Johnston MG, Hayashi A, Nelson W. Decreased lymphatic pumping after intravenous endotoxin administration in sheep. *Am J Physiol*. 1987; 253:H1349–H1357. [PubMed: 3425736]
17. Wee JL, Greenwood DL, Han X, Scheerlinck JP. Inflammatory cytokines IL-6 and TNF- $\alpha$  regulate lymphocyte trafficking through the local lymph node. *Vet Immunol Immunopathol*. 2011; 144:95–103. [PubMed: 21839522]
18. He C, Young AJ, West CA, Su M, Konerding MA, Mentzer SJ. Stimulation of regional lymphatic and blood flow by epicutaneous oxazolone. *J Appl Physiol*. 2002; 93:966–973. [PubMed: 12183492]
19. Worm AN, Rossing D. Microvascular protein leakage in extensive skin diseases: aspects of the transport mechanisms. *J Invest Dermatol*. 1980; 75:302–305. [PubMed: 6448904]
20. Staberg B, Klemp P, Aasted M, Worm AM, Lund P. Lymphatic albumin clearance from psoriatic skin. *J Am Acad Dermatol*. 1989; 9:857–861. [PubMed: 6643784]
21. Zhou Q, Wood R, Schwarz EM, Wang Y-J, Xing L. Near infrared lymphatic imaging demonstrates the dynamics of lymph flow and lymphangiogenesis during the acute vs. chronic phases of arthritis in mice. *Arthritis Rheum*. 2010; 62:1881–1889. [PubMed: 20309866]
22. von der Weid PY, Muthuchamy M. Regulatory mechanisms in lymphatic vessel contraction under normal and inflammatory conditions. *Pathophysiol*. 2009; 17:263–276.
23. Gopee NV, Cui Y, Olson G, Warbritton AR, Miller BJ, Couch LH, Warner WG, Howard PC. Response of mouse skin to tattooing: use of SKH-1 mice as surrogate model for human tattooing. *Toxicol Appl Pharmacol*. 2005; 209:145–158. [PubMed: 15913690]
24. Daviaud D, Boucher J, Gesta S, Dray C, Guigne C, Quilliot D, Ayav A, Ziegler O, Carpenne C, Saulnier-Blache J-S, Valet P, Castan-Laurell I. TNF- $\alpha$  up-regulates apelin expression in human and mouse adipose tissue. *The FASEB Journal*. 2006; 20:1528–1530.
25. Katagiri H, Ito Y, Ito S, Murata T, Yukihiro S, Narumiya S, Watanabe M, Majima M. TNF- $\alpha$  induces thromboxane receptor signaling-dependent microcirculatory dysfunction in mouse liver. *Shock*. 2008; 30:463–467. [PubMed: 18800000]
26. Croker BA, Krebs DL, Zhang J-G, Wormald S, Willson TA, Stanley EG, Robb L, Greenhalgh CJ, Forster I, Clausen BE, Nicola NA, Metcalf D, Hilton DJ, Roberts AW, Alexander WS. SOCS3 negatively regulates IL-6 signaling *in vivo*. *Nat Immunol*. 2003; 4:540–545. [PubMed: 12754505]
27. Bethin KE, Vogt SK, Muglia LJ. Interleukin-6 is an essential, corticotropin-releasing hormone-independent stimulator of the adrenal axis during immune system activation. *PNAS*. 2000; 97:9317–9322. [PubMed: 10922080]

28. Campbell JS, Prichard L, Schaper F, Schmitz J, Stephenson-Famy A, Rosenfeld ME, Argast GM, Heinrich PC, Fausto N. Expression of suppressors of cytokine signaling during liver regeneration. *J Clin Invest.* 107:1285–1292. 200. [PubMed: 11375418]
29. Kimura H, Ishibashi T, Shikama Y, Okano A, Akiyama Y, Uchida T, Maruyama Y. Interleukin-1 beta (IL-1 beta) induces thrombocytosis in mice: possible implication of IL-6. *Blood.* 1990; 76:2493–2500. [PubMed: 2265245]
30. Bani MR, Garofalo A, Scanziani E, Giavazzi R. Effect of interleukin-1-beta on metastasis formation in different tumor systems. *J Natl Cancer Inst.* 1991; 83:119–123. [PubMed: 1988686]
31. Tong Y, Tucker SB. Normal mouse skin lymphocyte, Langerhans cell, and keratinocyte responses to intradermal injections of interferon-alpha and interferon-gamma. *J Interferon Cytokine Res.* 1995; 15:235–241. [PubMed: 7584669]
32. Suda T, Callahan RJ, Wilkenson RA, van Rooijen N, Scheeberger EE. Interferon- reduces 1a+ dendritic cell traffic to the lung. *J Leukocyte Biol.* 1996; 60:519–526. [PubMed: 8864137]
33. Rutenfranz I, Kirchner H. Pharmacokinetics of recombinant murine interferon-gamma in mice. *J Interferon Res.* 1988; 8:573–580. [PubMed: 3148668]
34. Kim HS, Chung DH. TLR4-mediated IL-12 production enhances IFN- and IL-1 , which inhibits TGF- production and promotes antibody-induced joint inflammation. *Arthritis Res & Ther.* 2012; 14:R210–R222. [PubMed: 23036692]
35. Maus U, Huwe J, Maus R, Seeger W, Lohmeyer J. Alveolar JE/MCP-1 and endotoxin synergize to provoke lung cytokine upregulation, sequential neutrophil and monocyte influx, and vascular leakage in mice. *Am J Respir Crit Care Med.* 2001; 164:406–411. [PubMed: 11500341]
36. Wang H, Peters T, Kess D, Sindrilaru A, Oreshkova T, Rooijen NV, Stratis A, Renki AC, Sunderkotter C, Wiaschek M, Haase I, Scharffetter-Kochanek K. Activated macrophages are essential in a murine model for T cell-mediated chronic psoriasiform skin inflammation. *J Clin Invest.* 2006; 116:2105–2114. [PubMed: 16886059]
37. Matsukawa A, Hogaboam CM, Lukacs NW, Lincoln PM, Strieter RM, Kunkel SL. Endogenous monocyte chemoattractant protein-1 (MCP-1) protects mice in a model of acute septic peritonitis: cross-talk between MCP-1 and leukotriene B<sub>4</sub>. *J Immunol.* 1999; 163:6148–6154. [PubMed: 10570305]
38. Lee WY, Lockniskar MF, Fischer SM. Interleukin-1 mediates phorbol ester-induced inflammation and epidermal hyperplasia. *FASEB J.* 1994; 8:1081–1087. [PubMed: 7926375]
39. Johnson CS, Keckler DJ, Topper MI, Braunschweiger PG, Furmanski P. In vivo hematopoietic effects of recombinant interleukin-1 alpha in mice: stimulation of granulocytic, monocytic, megakaryocytic, and early erythroid progenitors, suppression of late-stage erythropoiesis, and reversal of erythroid suppression with erythropoietin. *Blood.* 1989; 73:678–683. [PubMed: 2783864]
40. Czuprynski DJ, Brown JF. Recombinant murine interleukin-1 alpha enhancement of nonspecific antibacterial resistance. *Infect Immun.* 1987; 55:2061–2065. [PubMed: 3497878]
41. Wright K, Morgan ET. Regulation of cytochrome P450IIC12 expression by interleukin-1 alpha, interleukin-6, and dexamethasone. *Mol Pharmacol.* 1991; 39:468–474. [PubMed: 2017147]
42. Uzarski J, Drelles MB, Gibbs SE, Ongstad EL, Goral JC, McKeown KK, Raehl AM, Roberts MA, Pytowski B, Smith MR, Goldman J. The resolution of lymphedema by interstitial flow in the mouse tail skin. *Am J Physiol Heart Circ Physiol.* 2008; 294:H1326–H1334. [PubMed: 18203849]
43. Gao B, Wang Y, Tsan M-F. The heat sensitivity of cytokine-inducing effect of lipopolysaccharide. *J Leukocyte Biol.* 2006; 80:359–366. [PubMed: 16720829]
44. Majde JA. Endotoxin detection. *Immunology Today.* 1992; 13:328–329. [PubMed: 1510815]
45. Schwager I, Jungi TW. Effect of human recombinant cytokines on the induction of macrophage procoagulant activity. *Blood.* 1994; 83:152–160. [PubMed: 8274733]
46. Kaye SA, Louise CB, Boyd B, Lingwood CA, Obrig TG. Shiga toxin-associated hemolytic uremic syndrome: interleukin-1 beta enhancement of Shig toxin cytotoxicity toward human vascular endothelial cells in vitro. *Infect Immun.* 1993; 61:3886–3891. [PubMed: 8359910]
47. Chaitanya GV, Franks SE, Cromer W, Wells SR, Bienkowska M, Jennings MH, Ruddell A, Ando T, Want Y, Gu Y, Sapp M, Mathis JM, Jordan PA, Minagar A, Alexande JS. Differential cytokine

- responses in human and mouse lymphatic endothelial cells to cytokines in vitro. *Lymphat Res Biol.* 2010; 8:155–164. [PubMed: 20863268]
48. Williams MR, Kataoka N, Sakurai Y, Powers CM, Eskin SG, McIntire LV. Gene expression of endothelial cells due to interleukin-1 beta stimulation and neutrophil transmigration. *Endothelium.* 2008; 15:73–165. [PubMed: 18568947]
49. Ni CW, Hsieh HJ, Chao YJ, Wang DL. Interleukin-6-induced JAK2/STAT3 signaling pathway in endothelial cells is suppressed by hemodynamic flow. *Am J Physiol Cell Physiol.* 2004; 287:C771–C780. [PubMed: 15151905]
50. Dyson A, Bryan NS, Fernandez BO, Garcia-Saura M-R, Saijo F, Mongardon N, Rodriguez J, Singer M, Feelisch M. An integrated approach to assessing nitroso-redox balance in systemic inflammation. *Free Radic Biol Med.* 2011; 51:1137–1145. [PubMed: 21718783]
51. Ju TJ, Dan JM, Cho YJ, Park SY. Inhibition of inducible nitric oxide synthase attenuates monosodium urate-induced inflammation in mice. *Korean J Physiol Pharmacol.* 2011; 15:363–369. [PubMed: 22359474]
52. Granger, DN.; Senchenkova, E. Inflammation and the microcirculation, chapter 4. San Rafael, California: Morgan & Claypool Publishers; 2010.
53. Schmid-Schonbein GW. Nitric oxide (NO) side of lymphatic flow and immune surveillance. *Proc Natl Acad Sci USA.* 2012; 109:3–4. [PubMed: 22178757]
54. Marchetti C, Casasco A, Di Nucci A, Reguzzoni M, Rosso S, Piovella F, Calligaro A, Polak JM. Endothelin and nitric oxide synthase in lymphatic endothelial cells: immunolocalization in vivo and in vitro. *Anat Rec.* 1997; 248:490–497. [PubMed: 9268139]
55. Hagendoorn J, Padera TP, Kashiwagi S, Isaka N, Noda F, Lin MI, Huang PL, Sessa WC, Fukumura D, Jain RK. Endothelial nitric oxide synthase regulates microlymphatic flow via collecting lymphatics. *Circ Res.* 2004; 95:204–209. [PubMed: 15192027]
56. Triggle CR, Samuel SM, Ravishankar S, Marei I, Arunachalam G, Ding H. The endothelium: influencing vascular smooth muscle in many ways. *Can J Physiol Pharmacol.* 2012; 90:713–738. [PubMed: 22625870]
57. Sawa Y, Ueki T, Hata M, Iwasawa K, Tsuruga E, Kojima H, Ishikawa H, Yoshida S. LPS-induced IL-6, IL-8, VCAM-1, and ICAM-1 expression in human lymphatic endothelium. *J Histochem Cytochem.* 2008; 56:97–109. [PubMed: 17938282]
58. Garrafa E, Imberti L, Tiberio G, Prandini A, Giulini SM, Caimi L. Heterogeneous expression of toll-like receptors in lymphatic endothelial cells derived from different tissues. *Immunol Cell Biol.* 2011; 89:475–481. [PubMed: 20921966]
59. Chakraborty S, Nepiyushchikh Z, Davis MJ, Zawieja DC, Muthuchamy M. Substance P activates both contractile and inflammatory pathways in lymphatics through the neurokinin receptors NK1R and NK3R. *Microcirculation.* 2011; 18:24–35. [PubMed: 21166923]
60. Lobov GI, Pan'kova MN. Heparin inhibits contraction of smooth muscle cells in lymphatic vessels. *Bull Exp Biol Med.* 2010; 149:4–6. [PubMed: 21113444]
61. von der Weid PY, Rehal S, Dyrda P, Lee S, Mathias R, Rahman M, Roizes S, Imtiaz MS. Mechanisms of VIP-induced inhibition of the lymphatic vessel pump. *J Physiol.* 2012; 590:2677–2691. [PubMed: 22451438]
62. Muthuchamy M, Zawieja D. Molecular Regulation of Lymphatic Contractility. *Ann NY Acad Sci.* 2008; 1131:89–99. [PubMed: 18519962]
63. Lukacs-Kornek V, Malhotra D, Fletcher AL, Acton SE, Elpek KG, Tayalia P, Collier AR, Turley SJ. Regulated release of nitric oxide by nonhematopoietic stroma controls expansion of the activated T cell pool in lymph nodes. *Nat Immunol.* 2012; 12:1096–1104. [PubMed: 21926986]
64. Bohlen HG, Gasheva OY, Zawieja DC. Nitric oxide formation by lymphatic bulb and valves is a major regulatory component of lymphatic pumping. *Am J Physiol Heart Circ Physiol.* 2011; 301:H1897–H1906. [PubMed: 21890688]
65. von der Weid PY, Zhao J, van Helden DF. Nitric oxide decreases pacemaker activity in lymphatic vessels of guinea pig mesentery. *Am J Physiol Heart Circ Physiol.* 2001; 280:H2707–H2716. [PubMed: 11356627]

66. Lewis RS, Kolesnik TB, Kuang Z, D’Cruz AA, Blewitt ME, Masters SL, Low A, Willson T, Norton RS, Nicholson SE. TLR regulation of SPSB1 controls inducible nitric oxide synthase induction. *J Immunol.* 2011; 187:3798–3805. [PubMed: 21876038]
67. Kunder CA, st. John AL, Li G, Leong KW, Berwin B, Staats HF, Abraham SN. Mast cell-derived particles deliver peripheral signals to remote lymph nodes. *J Exp Med.* 2009; 206:2455–2467. [PubMed: 19808250]
68. Soderberg KA, Payne GW, Sato A, Medzhitov R, Segal SS, Iwasaki A. Innate control of adaptive immunity via remodeling of lymph node feed arteriole. *PNAS.* 2005; 102:16315–16320. [PubMed: 16260739]
69. Liao S, Cheng G, Conner DA, Huang Y, Kucherlapati RS, Munn LL, Ruddle NH, Jain RK, Fukumura D, Padera TP. Impaired lymphatic contraction associated with immunosuppression. *Proc Natl Acad Sci USA.* 2011; 108:18784–18789. [PubMed: 22065738]
70. Margaritis KN, Black RA. Modelling the lymphatic system: challenges and opportunities. *J R Soc Interface.* 9:601–612. [PubMed: 22237677]
71. Aldrich MB, Guilliod R, Fife CE, Maus EA, Smith L, Rasmussen JC, Sevick-Muraca EM. Lymphatic abnormalities in the normal contralateral arms of subjects with breast cancer-related lymphedema as assessed by near-infrared fluorescent imaging. *Biomedical Optics Express.* 2012; 3:1256–1265. [PubMed: 22741072]
72. Mellor RH, Stanton AW, Azarbod P, Sherman MD, Levick JR, Mortimer PS. Enhanced cutaneous lymphatic network in the forearms of women with postmastectomy oedema. *J Vasc Res.* 2000; 37:501–512. [PubMed: 11146404]

### Highlights

- LPS administration results in systemic shutdown of lymphatic pumping
- TNF- and IL-1 singly can stop lymph movement systemically
- IL-1 's systemic effects on lymphatic function are mediated through iNOS

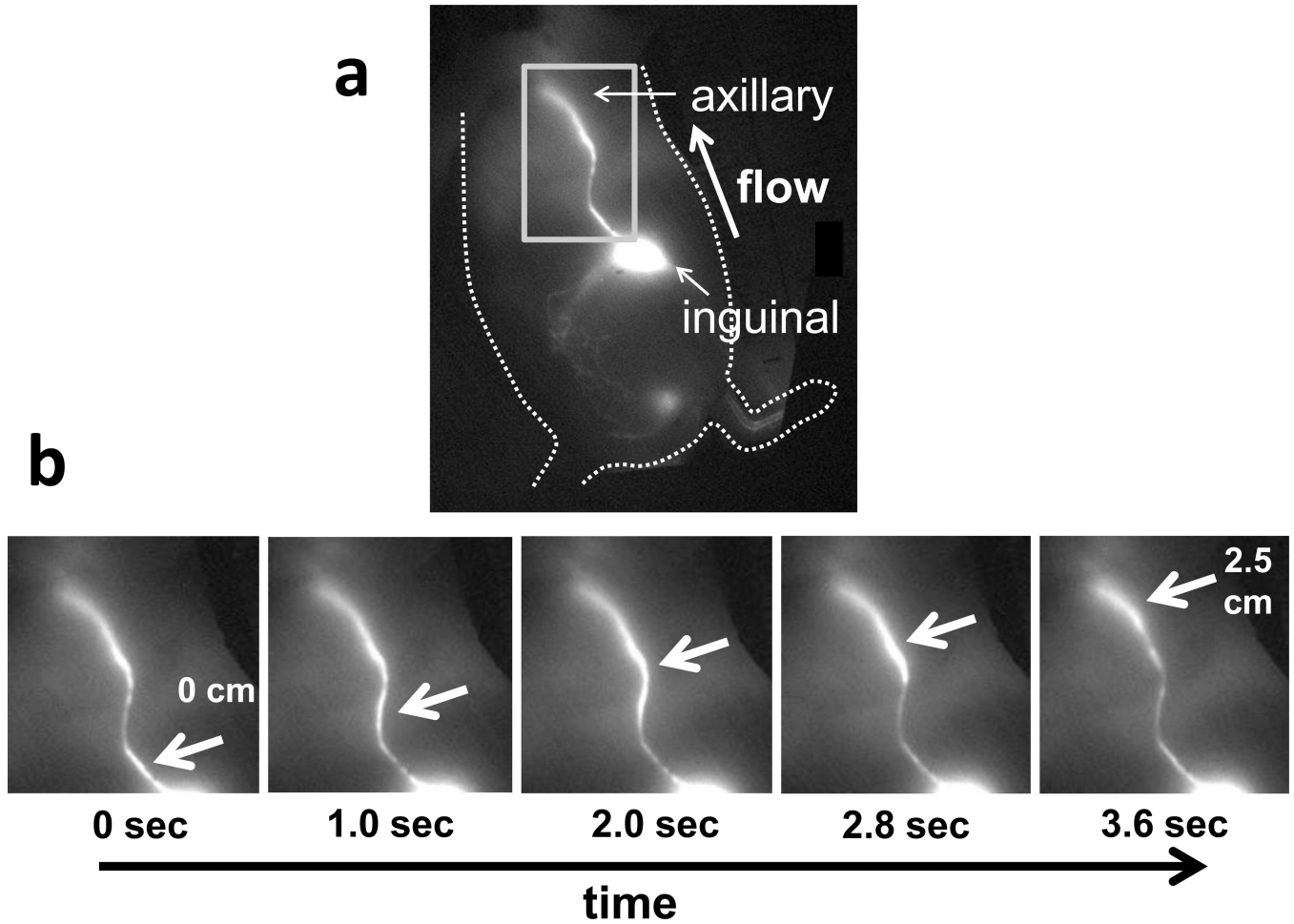


**Figure 1.**

(a) Fluorescent image of side of mouse, displaying inguinal-to-axillary collecting lymphatic vessel and direction of normal flow, and (b) typical images of lymphatic movement in a side view of a mouse. Panels show sequential images of rectangular area, with arrows pointing to lymph packet/bolus moving from the inguinal lymph node through a collecting lymphatic vessel up to the axillary region.

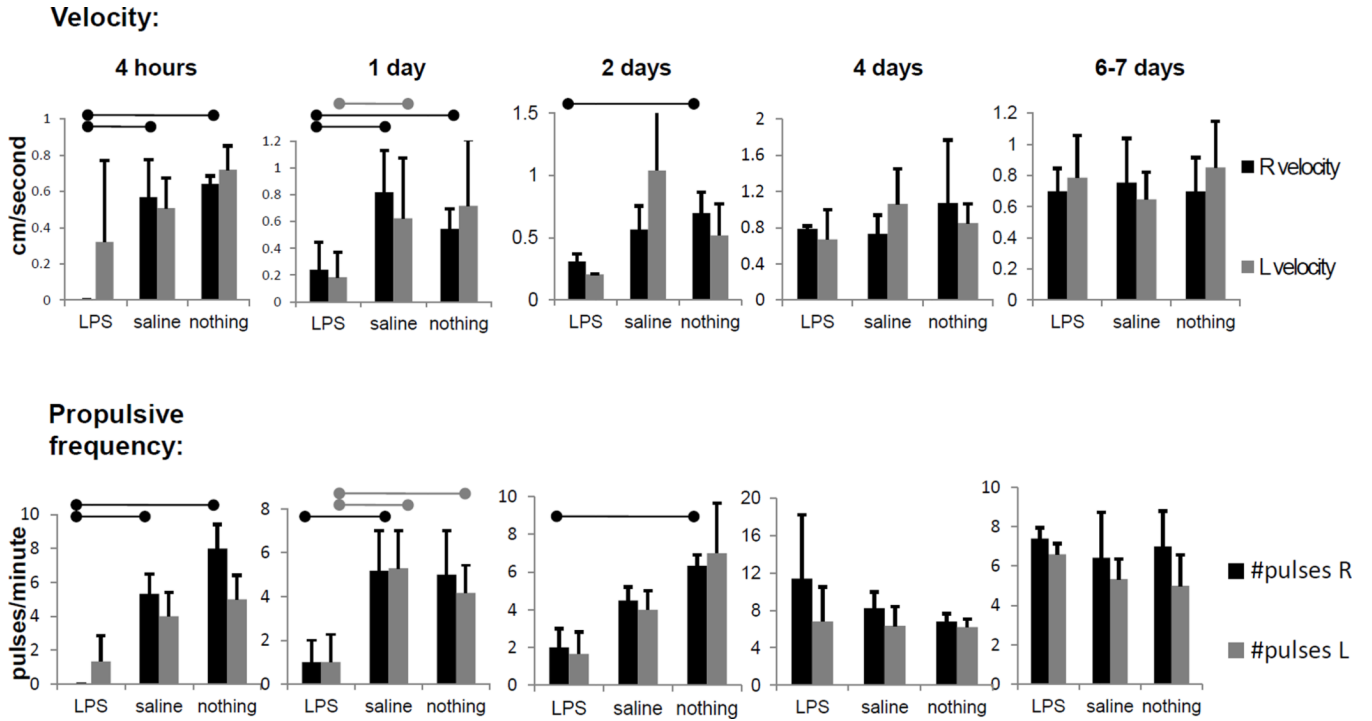


**Figure 2.** Lymphatic function decreased systemically and acutely in response to LPS administration. Pulsatile velocity, or centimeters per second, and propulsive frequency, or pulses per minute, in right-side and left-side inguinal-to-axillary lymphatic vessels at 4 hours, 1 day, 2 days, 4 days, and 7 days after intradermal LPS injection (100 µg/mouse), saline injection (20 µl) or no injection in dorsal aspect of right hind paw. n=4–7 mice per group. Bars over column graphs indicate p<0.05.



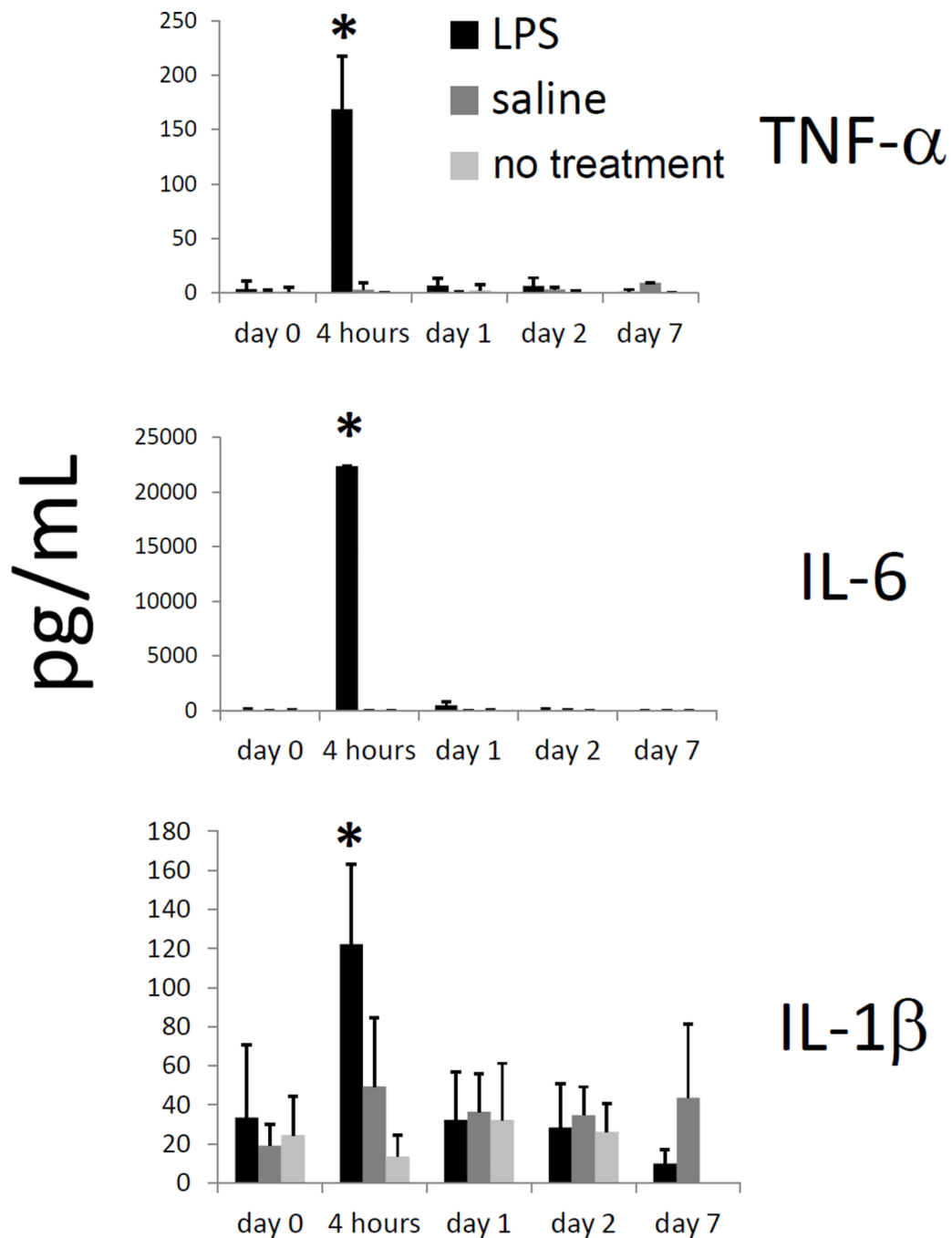


**Figure 3.**

TNF- $\alpha$ , IL-6, and IL-1 $\beta$  levels increase within 4 hours of LPS administration. TNF- $\alpha$ , IL-6, and IL-1 $\beta$  levels in mouse serum, as measured by Milliplex kit, at 0 hours, 4 hours, 1 day, 2 days, and 7 days after intradermal LPS (100  $\mu$ g/mouse), saline, or no injection in dorsal aspect of right hind paw. n=5 mice per group. \*=p<0.05 compared to saline or no injection.

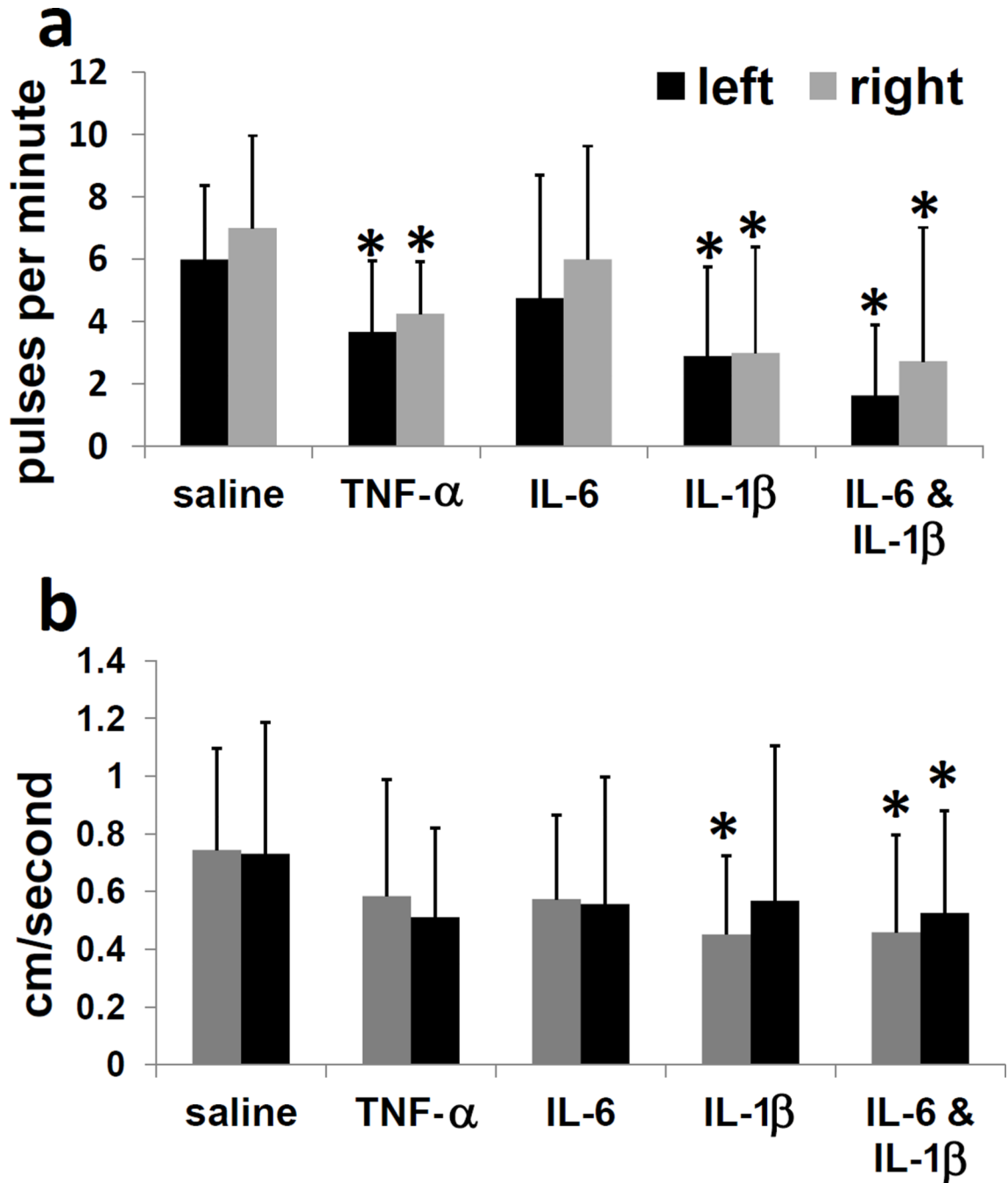


**Figure 4.**

Lymphatic function decreases systemically and acutely in response to administration of TNF- $\alpha$ , IL-6, and IL-1 $\beta$ . (a) Propulsive frequency, or pulses per minute, and (b) pulsatile velocity, or centimeters per second, in right-side and left-side inguinal-to-axillary lymphatic vessels at 4 hours after intradermal TNF- $\alpha$  (2  $\mu$ g/mouse), IL-6 (50 ng/mouse), IL-1 $\beta$  (1  $\mu$ g/mouse), or IL-6 plus IL-1 $\beta$  injection in dorsal aspect of right hind paw. n=10–16 mice per group. \*= $p$ <0.05 compared to saline.

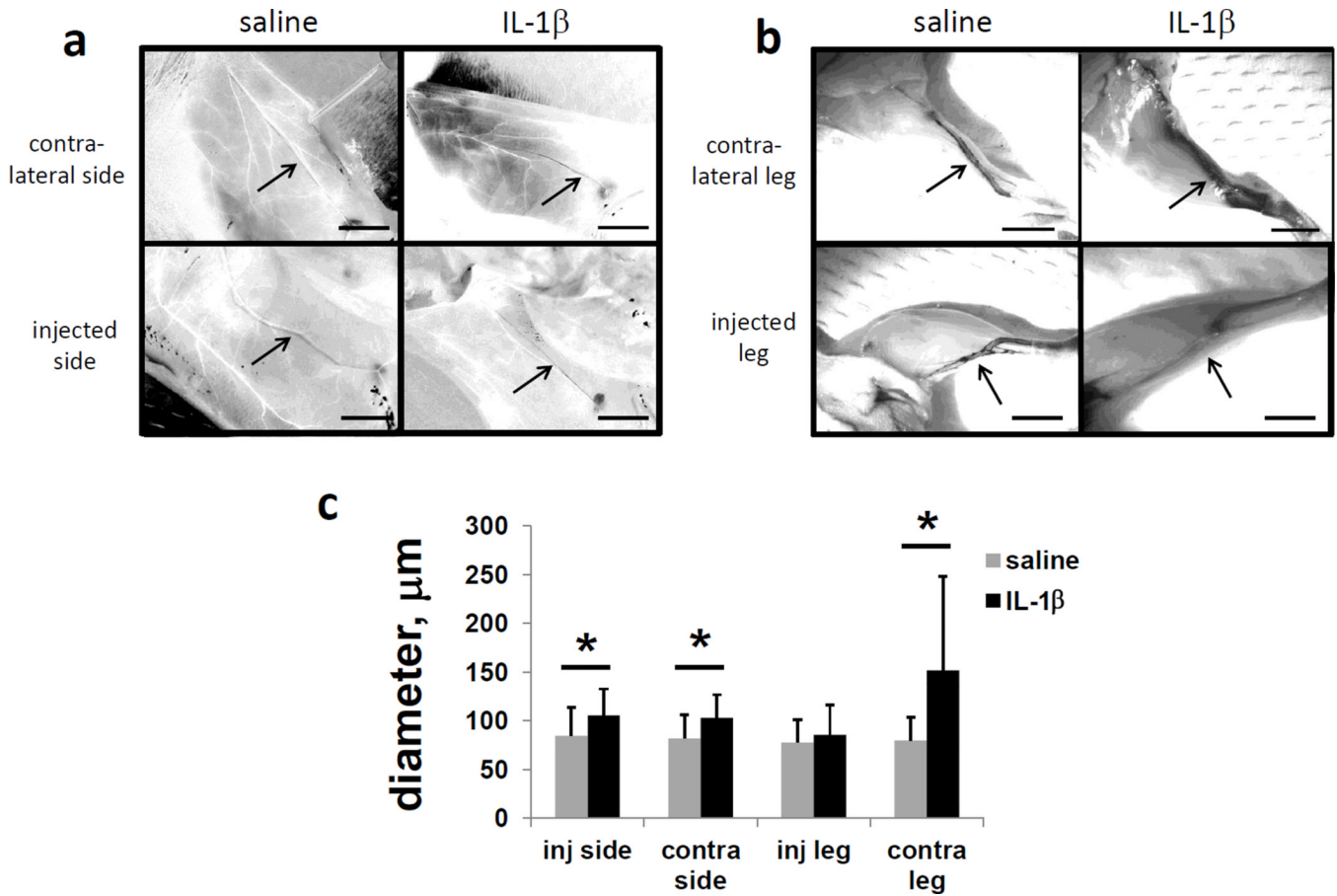


**Figure 5.** Hindlimb lymphatic vessels contralateral to IL-1 injection are dilated/leaky. Intravital images of inguinal-to-axillary and hindlimb lymphatic vessels stained with 1% Evan's blue dye injected i.d. in paws and at base of tail 4 hours after injection of saline or IL-1 (1  $\mu\text{g}$ /mouse) in the dorsal aspect of the right or left hind paw. (a) Inguinal-to-axillary lymphatic vessels, (b) hindlimb lymphatic vessels between paw and popliteal lymph nodes, and (c) average vessel diameters. After image conversion to HSB stack, lymphatic vessels appear black, and blood vessels appear white.  $n=10$  mice per group. Scale bars=5 mm.  $*=p<0.05$ . Images are representative of 10 mice per group.

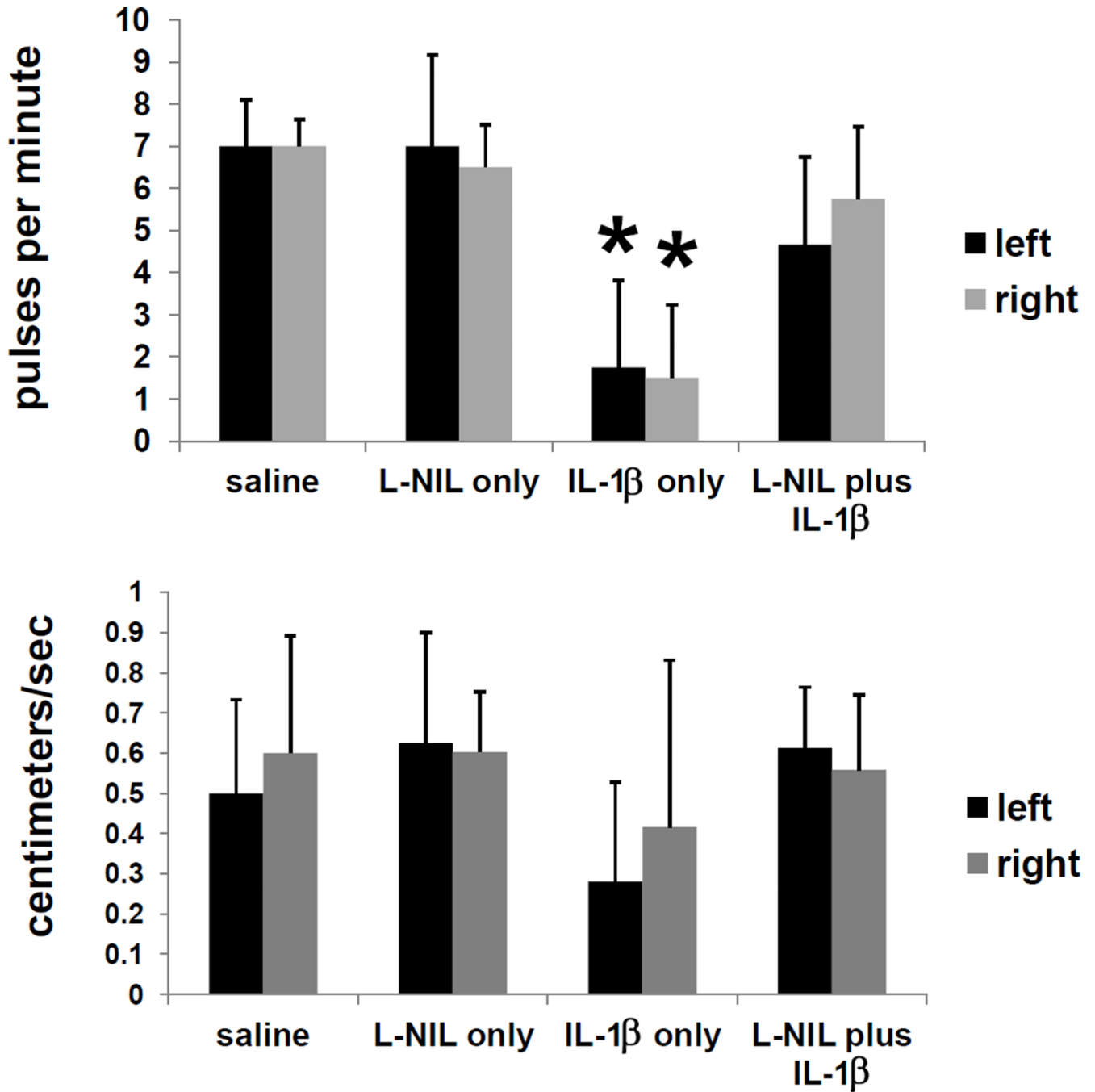


**Figure 6.**

Attenuation of the effects of IL-1 on lymphatic function by the iNOS inhibitor L-NIL. Pulsatile frequency and velocity in mice after iNOS inhibitor (L-NIL) treatment. Mice were injected with 200  $\mu$ g (i.p.) L-NIL or saline, then IL-1 (1  $\mu$ g/mouse, i.d. in dorsal aspect of right hind paw) or saline one hour later, and imaged with ICG four more hours later. n=6 mice per group. \*=p<0.05.